Alcohol-sourced acetate reduces T cell filamentous actin branching and migration

Vugar Azizov[1,2], Michael Frech[1,2], Jörg Hofmann[3], Marketa Kubankova[4], Dennis Lapuente[5], Matthias Tenbusch[5], Jochen Guck[4], Georg Schett[1,2], and Mario M. Zaiss[1,2] *

Affiliations:

[1]Department of Internal Medicine 3, Rheumatology and Immunology, Friedrich-Alexander-University Erlangen-Nürnberg and Universitätsklinikum Erlangen; Erlangen, Germany

[2]Deutsches Zentrum Immuntherapie (DZI), Friedrich-Alexander-University Erlangen-Nürnberg and Universitätsklinikum Erlangen; Erlangen, Germany

[3]Division of Biochemistry, Department of Biology, Friedrich-Alexander-University Erlangen-Nürnberg; Erlangen, Germany

[4]Max Planck Institute for the Science of Light & Max Planck Zentrum für Physik und Medizin; Erlangen, Germany

[5]Institute of Clinical and Molecular Virology, Friedrich-Alexander-University Erlangen-Nürnberg and Universitätsklinikum Erlangen; Erlangen, Germany

*Corresponding author: Email: mario.zaiss@uk-erlangen.de

Abstract: Alcohol is among the most widely consumed dietary substances. While excessive alcohol consumption damages the liver, heart and brain, clinical observations suggest that alcohol has strong immunoregulatory properties. Mechanisms by which alcohol undermines immune cell functions during autoimmunity and vaccination are currently elusive. Herein, we show that acetate, the main metabolite of alcohol, effectively inhibits the migratory capacity of T cells through acetylation of cortactin, a protein which stabilizes and promotes branching of filamentous actin. Acetate-induced cytoskeletal changes effectively inhibited activation, proliferation, and immune synapse formation in T cells at tissue concentrations reached by alcohol consumption. In summary, these data show that acetate inhibits T cell-mediated immune responses by modulating the T cell cytoskeletal biomechanics.

One-Sentence Summary: Exposure to elevated acetate concentrations change T cell biomechanics, reducing cell migration and immune synapse formation.

Main Text: Multiple studies have shown detrimental effects of alcohol consumption on human health (*1*). In contrast, several clinical studies have demonstrated a correlation between autoimmune disease severity and moderate to high alcohol consumption (*2*). In an effort to better understand alcohol's effect on autoimmunity, we have shown that alcohol consumption mitigates T cell dependent humoral immune responses in preclinical rheumatoid arthritis (RA) and vaccination models (*3*). Because alcohol is rapidly metabolized to acetate and acetate can contribute to protein acetylation, we studied the effect of direct acetate supplementation on immune responses (*3*, *4*). Of interest, our findings in both alcohol-fed and acetate-fed mice matched those observed following pharmacological HDAC6 inhibition in a preclinical model of systemic lupus erythematosus (SLE), such as decreased autoantibody titers, germinal center (GC) infiltration by Tfh cells and downregulated Bcl6, PD-1 and IL-21 as characteristic Tfh gene and functional markers (*5*, *6*). HDAC6 is the major deacetylase of cytoskeletal proteins and has been shown to be required for immune synapse formation (*7*). The T cell cytoskeleton needs to be highly dynamic to meet the requirements of scanning for antigens, forming an immune synapse, activation, and migration (*8*, *9*). Based on the importance of HDAC6's and acetate's potential to increase protein acetylation, we set out to investigate whether there is a link between acetate exposure and mitigation of cytoskeletal dynamics leading to reduced T cell dependent immune responses.

Building upon our published results, we ventured to study whether the decreased infiltration of GCs by T and B cells along with reduced Tfh-B cell contacts was due to cytoskeletal deficiencies following alcohol-sourced acetate exposure (*3*). First, we set to quantify the exposure of T cells to acetate upon alcohol consumption by measuring acetate levels in alcohol-impacted and immune relevant lymphoid tissues such as the liver, inguinal lymph node (iLN), and spleen of alcohol-fed mice. We found that acetate indeed accumulates in these organs, especially in lymphoid organs reaching concentrations surpassing 5 mM (fig. S1A-C). Next, we quantified whether or not exposure to 5 mM acetate concentration results in incorporation to cellular metabolism. Previously it was shown that increased in vivo ethanol concentration can lead to an increase in intracellular acetate and citrate (*4*). In an in vitro treatment of mouse naïve $CD4^+$ $CD25^-$ $CD44^{low}$ $CD62L^{high}$ T cells, hereafter naïve $CD4^+$ T cells, with ^{13}C labelled acetate, we were able to confirm an increase in ^{13}C containing citrate (fig. S1D). In a subsequent quantification of histone 3 (H3) acetylation levels in the same $CD4^+$ T cells, we observed increased H3 acetylated at lysine 27 (fig. S1E). Together, these findings confirm increased exposure of T cells to acetate, leading to increased protein acetylation within cells. We next performed a trans-well migration assay of either mouse $CD4^+$ or human Jurkat T cells in the presence and absence of acetate. Here we found a significant decrease in trans-well migration of mouse and human derived $CD4^+$ T cells (Fig. 1A, 1B). To study the potential impact of decreased T cell migration in vivo, primary mouse $CD4^+$ T cells were pre-treated for 4 hours with 5 mM acetate in vitro, loaded with CellTrace® dye and combined at 1:1 ratio of control to acetate treated $CD4^+$ T cells, to a total of 6×10^7 cells. We, then, adoptively transferred 6×10^7 cells to recipient C57BL/6 wildtype naïve mice not supplemented with alcohol. 2 hours post adoptive transfer, we observed about 50% decrease in migration of acetate treated $CD4^+$ T cells to spleens of recipient mice compared to control $CD4^+$ T cells (Fig. 1C). The same observation was true at 48 hours post adoptive transfer (Fig. 1D). T cells require a dynamic cytoskeleton, especially rapid modifications of filamentous actin (F-Actin), for migration, immune synapse formation and activation (*10*). Upon quantification of total F-Actin levels by Alexa-Fluor-488™-conjugated phalloidin staining and flow cytometry analysis in mouse naïve $CD4^+$ T cells exposed to 5 mM acetate, we found a dose dependent decrease of F-Actin median fluorescence intensity

(MFI) (Fig. 2A). F-Actin deficiency also manifests itself by increased cell deformability measured by real-time deformability cytometry (RT-DC) (*11*,*12*). We performed RT-DC and found an increase in T cell deformability upon acetate exposure (Fig. 2B and S2). A recent review article by Mu et al. summarized the acetylation of various components of the cytoskeleton (*13*). We identified cortactin, a facilitator and stabilizer of F-Actin branching, as a likely candidate for further research as it has acetylation site in each of its 6.5 repeat regions within the actin-filament binding domain (ABD) (*13*). Most notably, cortactin is also a direct target of HDAC6 (*13*, *14*). As pointed out before, treatment of C57BL/6 mice with HDAC6 inhibitor reduced disease severity in a SLE preclinical model and akin to our findings with acetate-exposed collagen induced arthritis (CIA) and T cell dependent vaccination mouse models (*3*, *5*, *6*). Cortactin acetylation leads to decreased binding to F-Actin and subsequent F-Actin branching (*13*). Acetate treatment of Jurkat T cells increased acetylation levels of cortactin (fig. S3A). Because acetylation of cortactin prevents its binding to F-Actin, we mutated lysine residues to arginine residues at the acetylation sites (CTTN_KR) within cortactin ABD (*14*). Microscopy analysis of F-Actin MFI in Jurkat T cells overexpressing CTTN_KR exhibited increased F-Actin amounts even in the presence of acetate (fig. S3B). Further analysis of F-Actin-bound cortactin by Förster Resonance Energy Transfer (FRET) revealed reduced F-Actin-bound cortactin levels upon acetate treatment, and that Jurkat T cells expressing mutated cortactin (CTTN_KR) were resistant to such reduction (Fig. 3A). Further, we also quantified acetate's effect on cortactin-F-Actin binding in HEK293T cells and found a similar result (fig. S3C). Next, in trans-well migration assays we found that the expression of acetylation resistant cortactin (CTTN_KR) rescued acetate induced migration deficiency (Fig. 3B). Modifications to F-Actin are required for lamellipodia formation and proper T cell migration (*10*). For this reason, we performed 2D Jurkat T cell tracking in cell culture treated wells by live-cell microscopy. We found that acetate treated Jurkat T cells had a reduced linearity of forward progression and directional change rate, and that cells expressing acetylation resistant cortactin (CTTN_KR) were resistant to the effects of acetate (fig. S3D-F). In order to better study the highly dynamic lamellipodia formation, we generated Jurkat T cells expressing LifeAct-mScarlet-i_N1, a short peptide that binds F-Actin. Here too, we observed reduced lamellipodia formation upon acetate treatment of Jurkat T cells (Fig. 3C-D and Movie S1). Finally, Western Blot analysis of the splenocytes isolated from alcohol-fed mice exhibited increased levels of acetylated cortactin in comparison to water-fed, control mice (fig. S3G). This finding indicates that alcohol consumption can directly increase acetylation of cortactin in secondary lymphoid organs such as spleen. In summary, increased acetate, as shown here as a result of alcohol consumption, accumulates in lymphoid organs, increase cellular acetylated-cortactin, prevent F-Actin branching and hinder T cell migration capacity (Fig. 4). F-Actin cytoskeleton is required for T cell – antigen presenting cell (APC) interaction and immune synapse formation (*15–17*). Therefore, we performed co-culturing experiment of NP-CGG antigen-pulsed dendritic cells (DCs) and $CD4^+$ T cells in order to interrogate if acetate-directed F-Actin deficiency affects T cell activation. T cells were either pre-treated with 5 mM acetate or vehicle, while antigen-pulse of DCs with NP-CGG was performed in an absence of acetate. Later upon combining DCs and T cells, acetate treatment was continued in an effort to replicate in vivo acetate exposure within lymphoid organs. Here, flow cytometry analysis revealed reduced surface CD69 levels on acetate treated $CD4^+$ $CD25^+$ T cells indicating reduced activation (fig. S4A). In the same experiment, flow cytometry analysis of acetate treated $CD4^+$ T cells revealed that Ki67 levels, a proliferation marker, were reduced (fig. S4B). Taken together these experiments exhibit deficiencies in T cell activation and proliferation. Next, we performed confocal fluorescence microscopy to visualize F-Actin at the immune synapse by phalloidin staining and quantified

MFI values. There was a decrease in F-Actin accumulation at the immune synapses within T cells between T cells and DCs (fig. S4C). Activation of naïve $CD4^+$ T cells with anti-CD3 and anti-CD28 antibody coated beads in the presence of acetate also resulted in reduced F-Actin amounts, as quantified by Alexa-Fluor-488™-phalloidin MFI (fig. S4D). These experiments document the sensitivity of T cells to cytoskeletal deficiencies for migration, immune synapse formation, and activation, and they shed light on our previously published finding of reduced Tfh-B cell conjugate formation upon acetate exposure in vivo and in vitro (*3*).

The Arp2/3 complex is another major F-Actin branching nucleator (*17*). But it does require cortactin to facilitate its binding to F-Actin. Whereas cortactin was shown to increase the affinity of Arp2/3 complex for F-Actin by almost 20-fold (*18*). In addition, cortactin plays a key role in linking cortical F-Actin to the cell membrane (*19*). Inhibition of Arp2/3 complex formation reduced T cell deceleration upon encountering high affinity antigens to a level observed for low affinity antigens (*20*). This finding potentially explains the weak immune synapse formation in our current study and also reduced T-B cell conjugate formation upon acetate exposure in our previously published findings (*3*). $CD4^+$ and $CD8^+$ T cell migration patterns through secondary lymphoid organs (SLOs) differ, $CD4^+$ T cells spend more time probing MHCII molecules presented on DCs and are significantly faster in entering and exiting SLOs than $CD8^+$ T cells (*21–23*). It is possible that diminished F-Actin branching can therefore mitigate TCR coupling with high-affinity antigens and reduce T cell arrest and subsequent activation. Interestingly, in a mouse model of type 1 diabetes, mice fed with acetate-yielding chow exhibited a reduction in autoreactive T cells (both $CD4^+$ and $CD8^+$) and ultimately reduced the incidence of the disease (*24*). In another study of experimental autoimmune encephalomyelitis (EAE), cortactin knock-out mice exhibited decreased incidence, disease severity, and infiltration of the central nervous system by $CD4^+$ T cells (*25*). Interestingly, we observed the same effect in alcohol-fed EAE mice (*3*). In an influenza infection model, alcohol-fed mice exhibited decreased homing to lungs, reduced CD69, CD103, and CXCR3 positive tissue resident $CD8^+$ T cells (fig. S5). Cortactin is overexpressed in B cells of chronic lymphoblastic leukemia patients (CLL), implicated in T cell acute lymphoblastic leukemia (T-ALL), and promotes migration in cancer (*26*, *27*). Identification of an Achille's heal of T cell migration, motility, and immune synapse formation can set the stage for pharmacological and/or natural targeting in cases of autoimmunity. Further, such interventions can also help improve immune responses to vaccinations. In an evolutionary perspective, hominids adapted to alcohol metabolism by feeding on fermenting fruits from the forest floor (*28*). It is possible that indirect alcohol consumption mitigated adverse immune responses in early humans under high microbial load. Today, we see the same effects reflected as mitigation of autoimmunity amongst alcohol consumers.

References and Notes

1. M. A. Schuckit, Alcohol-use disorders. *Lancet*. 373, 492–501 (2009).
2. V. Azizov, M. M. Zaiss, Alcohol Consumption in Rheumatoid Arthritis: A Path through the Immune System. *Nutrients*. 13, 1324 (2021).
3. V. Azizov, K. Dietel, F. Steffen, K. Dürholz, J. Meidenbauer, S. Lucas, M. Frech, Y. Omata, N. Tajik, L. Knipfer, A. Kolenbrander, S. Seubert, D. Lapuente, M. V. Sokolova, J. Hofmann, M. Tenbusch, A. Ramming, U. Steffen, F. Nimmerjahn, R. Linker, S. Wirtz, M. Herrmann, V. Temchura, K. Sarter, G. Schett, M. M. Zaiss, Ethanol consumption inhibits TFH cell responses and the development of autoimmune arthritis. *Nat Commun*. 11, 1998 (2020).
4. P. Mews, G. Egervari, R. Nativio, S. Sidoli, G. Donahue, S. I. Lombroso, D. C. Alexander, S. L. Riesche, E. A. Heller, E. J. Nestler, B. A. Garcia, S. L. Berger, Alcohol metabolism contributes to brain histone acetylation. *Nature*. 574, 717–721 (2019).
5. J. Ren, M. D. Catalina, K. Eden, X. Liao, K. A. Read, X. Luo, R. P. McMillan, M. W. Hulver, M. Jarpe, P. Bachali, A. C. Grammer, P. E. Lipsky, C. M. Reilly, Selective Histone Deacetylase 6 Inhibition Normalizes B Cell Activation and Germinal Center Formation in a Model of Systemic Lupus Erythematosus. *Front Immunol*. 10, 2512 (2019).
6. N. L. Regna, M. D. Vieson, X. M. Luo, C. B. Chafin, A. G. Puthiyaveetil, S. E. Hammond, D. L. Caudell, M. B. Jarpe, C. M. Reilly, Specific HDAC6 inhibition by ACY-738 reduces SLE pathogenesis in NZB/W mice. *Clin Immunol*. 162, 58–73 (2016).
7. J. M. Serrador, J. R. Cabrero, D. Sancho, M. Mittelbrunn, A. Urzainqui, F. Sánchez-Madrid, HDAC6 Deacetylase Activity Links the Tubulin Cytoskeleton with Immune Synapse Organization. *Immunity*. 20, 417–428 (2004).
8. D. J. Fowell, M. Kim, The spatio-temporal control of effector T cell migration. *Nat Rev Immunol*. 21, 582–596 (2021).
9. M. Mastrogiovanni, M. Juzans, A. Alcover, V. D. Bartolo, Coordinating Cytoskeleton and Molecular Traffic in T Cell Migration, Activation, and Effector Functions. *Frontiers Cell Dev Biology*. 8, 591348 (2020).
10. L. Dupré, R. Houmadi, C. Tang, J. Rey-Barroso, T Lymphocyte Migration: An Action Movie Starring the Actin and Associated Actors. *Front Immunol*. 6, 586 (2015).
11. S. Golfier, P. Rosendahl, A. Mietke, M. Herbig, J. Guck, O. Otto, High-throughput cell mechanical phenotyping for label-free titration assays of cytoskeletal modifications. *Cytoskeleton*. 74, 283–296 (2017).
12. O. Otto, P. Rosendahl, A. Mietke, S. Golfier, C. Herold, D. Klaue, S. Girardo, S. Pagliara, A. Ekpenyong, A. Jacobi, M. Wobus, N. Töpfner, U. F. Keyser, J. Mansfeld, E. Fischer-Friedrich, J. Guck, Real-time deformability cytometry: on-the-fly cell mechanical phenotyping. *Nature Methods*. **12**, 199–202 (2015).
13. M. A, C. J. Latario, L. E. Pickrell, H. N. Higgs, Lysine acetylation of cytoskeletal proteins: Emergence of an actin code. *J Cell Biol*. 219, e202006151 (2020).

14. X. Zhang, Z. Yuan, Y. Zhang, S. Yong, A. Salas-Burgos, J. Koomen, N. Olashaw, J. T. Parsons, X.-J. Yang, S. R. Dent, T.-P. Yao, W. S. Lane, E. Seto, HDAC6 Modulates Cell Motility by Altering the Acetylation Level of Cortactin. *Mol Cell*. 27, 197–213 (2007).
15. S. Valitutti, M. Dessing, K. Aktories, H. Gallati, A. Lanzavecchia, Sustained signaling leading to T cell activation results from prolonged T cell receptor occupancy. Role of T cell actin cytoskeleton. *J Exp Medicine*. 181, 577–584 (1995).
16. H. Colin-York, Y. Javanmardi, M. Skamrahl, S. Kumari, V. T. Chang, S. Khuon, A. Taylor, T.-L. Chew, E. Betzig, E. Moeendarbary, V. Cerundolo, C. Eggeling, M. Fritzsche, Cytoskeletal Control of Antigen-Dependent T Cell Activation. *Cell Reports*. 26, 3369-3379.e5 (2019).
17. M. Fritzsche, R. A. Fernandes, V. T. Chang, H. Colin-York, M. P. Clausen, J. H. Felce, S. Galiani, C. Erlenkämper, A. M. Santos, J. M. Heddleston, I. Pedroza-Pacheco, D. Waithe, J. B. de la Serna, B. C. Lagerholm, T. Liu, T.-L. Chew, E. Betzig, S. J. Davis, C. Eggeling, Cytoskeletal actin dynamics shape a ramifying actin network underpinning immunological synapse formation. *Sci Adv*. 3, e1603032 (2017).
18. T. Uruno, J. Liu, P. Zhang, Y. Fan, C. Egile, R. Li, S. C. Mueller, X. Zhan, Activation of Arp2/3 complex-mediated actin polymerization by cortactin. *Nat Cell Biol*. 3, 259–266 (2001).
19. S. A. Weed, J. T. Parsons, Cortactin: coupling membrane dynamics to cortical actin assembly. *Oncogene*. 20, 6418–6434 (2001).
20. H. D. Moreau, F. Lemaître, K. R. Garrod, Z. Garcia, A.-M. Lennon-Duménil, P. Bousso, Signal strength regulates antigen-mediated T-cell deceleration by distinct mechanisms to promote local exploration or arrest. *Proc National Acad Sci*. 112, 12151–12156 (2015).
21. J. N. Mandl, R. Liou, F. Klauschen, N. Vrisekoop, J. P. Monteiro, A. J. Yates, A. Y. Huang, R. N. Germain, Quantification of lymph node transit times reveals differences in antigen surveillance strategies of naïve CD4+ and CD8+ T cells. *Proc National Acad Sci*. 109, 18036–18041 (2012).
22. G. M. Fricke, K. A. Letendre, M. E. Moses, J. L. Cannon, Persistence and Adaptation in Immunity: T Cells Balance the Extent and Thoroughness of Search. *Plos Comput Biol*. 12, e1004818 (2016).
23. A. Gérard, G. Patino-Lopez, P. Beemiller, R. Nambiar, K. Ben-Aissa, Y. Liu, F. J. Totah, M. J. Tyska, S. Shaw, M. F. Krummel, Detection of Rare Antigen-Presenting Cells through T Cell-Intrinsic Meandering Motility, Mediated by Myo1g. *Cell*. 158, 492–505 (2014).
24. E. Mariño, J. L. Richards, K. H. McLeod, D. Stanley, Y. A. Yap, J. Knight, C. McKenzie, J. Kranich, A. C. Oliveira, F. J. Rossello, B. Krishnamurthy, C. M. Nefzger, L. Macia, A. Thorburn, A. G. Baxter, G. Morahan, L. H. Wong, J. M. Polo, R. J. Moore, T. J. Lockett, J. M. Clarke, D. L. Topping, L. C. Harrison, C. R. Mackay, Gut microbial metabolites limit the frequency of autoimmune T cells and protect against type 1 diabetes. *Nat Immunol*. 18, 552–562 (2017).

25. M. Samus, Y.-T. Li, L. Sorokin, K. Rottner, D. Vestweber, Actin-Binding Protein Cortactin Promotes Pathogenesis of Experimental Autoimmune Encephalomyelitis by Supporting Leukocyte Infiltration into the Central Nervous System. *J Neurosci*. 40, 1389–1404 (2020).
26. M. Schnoor, T. E. Stradal, K. Rottner, Cortactin: Cell Functions of A Multifaceted Actin-Binding Protein. *Trends Cell Biol*. 28, 79–98 (2018).
27. Y. Zhang, M. Zhang, H. Dong, S. Yong, X. Li, N. Olashaw, P. A. Kruk, J. Q. Cheng, W. Bai, J. Chen, S. V. Nicosia, X. Zhang, Deacetylation of cortactin by SIRT1 promotes cell migration. *Oncogene*. 28, 445–460 (2009).
28. M. A. Carrigan, O. Uryasev, C. B. Frye, B. L. Eckman, C. R. Myers, T. D. Hurley, S. A. Benner, Hominids adapted to metabolize ethanol long before human-directed fermentation. *Proc National Acad Sci*. 112, 458–463 (2015).
29. J. Schindelin, I. Arganda-Carreras, E. Frise, V. Kaynig, M. Longair, T. Pietzsch, S. Preibisch, C. Rueden, S. Saalfeld, B. Schmid, J.-Y. Tinevez, D. J. White, V. Hartenstein, K. Eliceiri, P. Tomancak, A. Cardona, Fiji: an open-source platform for biological-image analysis. *Nat Methods*. 9, 676–682 (2012).
30. J.-Y. Tinevez, N. Perry, J. Schindelin, G. M. Hoopes, G. D. Reynolds, E. Laplantine, S. Y. Bednarek, S. L. Shorte, K. W. Eliceiri, TrackMate: An open and extensible platform for single-particle tracking. *Methods*. 115, 80–90 (2017).
31. P. Müller, E. O'Connell, M. Schlögel, Shape-Out version 2.3.0: Analysis software for real-time deformability cytometry [Software]. Available at https://github.com/ZELLMECHANIK-DRESDEN/ShapeOut2. *Github* (2019).
32. P. Müller, E. O'Connell, M. Herbig, M. Schlögel, P. Rosendahl, dclab version 0.31.2: Python library for the post-measurement analysis of real-time deformability cytometry data sets. *GitHub* (2015).
33. D. S. Bindels, L. Haarbosch, L. van Weeren, M. Postma, K. E. Wiese, M. Mastop, S. Aumonier, G. Gotthard, A. Royant, M. A. Hink, T. W. Gadella Jr, mScarlet: a bright monomeric red fluorescent protein for cellular imaging. *Nat Methods*. 14 (1), 53–56 (2017).
34. S. Kempa, J. Hummel, T. Schwemmer, M. Pietzke, N. Strehmel, S. Wienkoop, J. Kopka, W. Weckwerth, An automated GCxGC-TOF-MS protocol for batch-wise extraction and alignment of mass isotopomer matrixes from differential 13C-labelling experiments: a case study for photoautotrophic-mixotrophic grown Chlamydomonas reinhardtii cells. *J. Basic Microbiol.* 49, 82-91 (2009)

Acknowledgments: We thank Schimpf M., Danzer H. and Steffen F. for technical assistance. We also thank Schmidt K. and Harrer T. for their help with T cell electroporation. We are grateful to Dürholz K., Schälter F., Saad M.S.A., Vogg M., Ramming A., Weidner D. for their support and help with experiments. We thank Geisberger S. and Kempa S. for ^{13}C Citrate quantification and data analysis. We thank Tripal P. Winter Z. and Schmidt B. from the OICE in Erlangen for technical expertise. We thank Mielenz D., Sarter K., and Brandl C., for helpful discussions.

Funding: VA, MF, GS and MMZ are funded by the Deutsche Forschungsgemeinschaft (DFG-FOR2886 project A1 and CRC1181 project B07), the Bundesministerium für Bildung und Forschung (BMBF; project MASCARA), the H2020 GA 810316 - 4D-Nanoscope ERC Synergy Project, the IMI funded projects RTCure and HIPPOCRATES, the Emerging Fields Initiative MIRACLE of the Friedrich-Alexander-Universität Erlangen-Nürnberg.

Author contributions:

Conceptualization: VA, GS, MMZ

Methodology: VA, MF, JH, MK, DL

Investigation: VA, MK, MT, MMZ

Visualization: VA, MF, MK

Funding acquisition: GS, MMZ

Project administration: VA, MMZ

Supervision: MMZ

Writing – original draft: VA, MMZ

Writing – review & editing: VA, MT, JG, GS, MMZ

Competing interests: Authors declare that they have no competing interests.

Data and materials availability: All data are available in the main text or the supplementary materials. pLifeAct_mScarlet_N1 was a gift from Dorus Gadella (Addgene plasmid # 85054; http://n2t.net/addgene:85054 ; RRID:Addgene_85054)

Supplementary Materials

Materials and Methods

Figs. S1 to S5

Movie S1

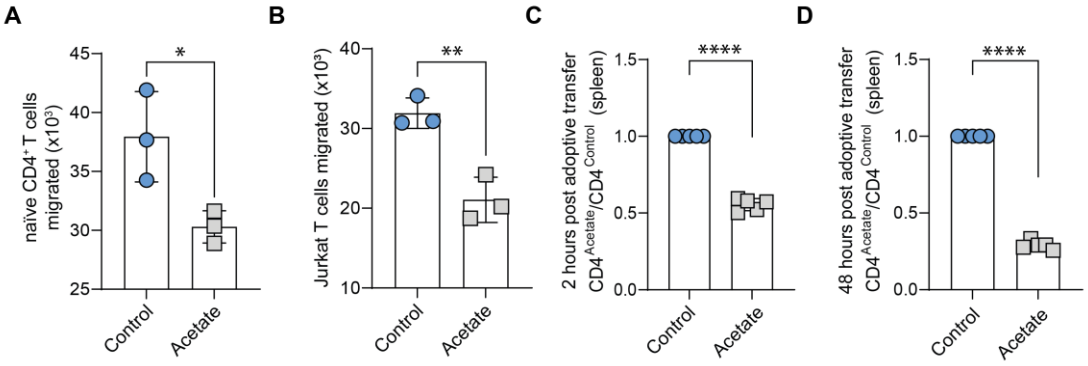

Fig. 1. Acetate exposed T cells exhibit reduced migration capacity in vitro and in vivo. (**A**) Numbers of migrated mouse naïve $CD4^+$ T cells and (**B**) Jurkat T cells in vitro trans-well assay, counted by flow cytometer. (**C**) The ratio of acetate to control treated mouse $CD4^+$ T cells found in the spleens of recipient mice in an adoptive transfer experiment at 2 hours and (**D**) 48 hours post transfer (each point represents one mouse, n = 5). Data shown from one of three independent experiments (A and B), two independent experiments (C and D) and expressed as mean ± SD. Statistical difference was determined by Students two-tailed t-test. *$p < 0.05$; **$p < 0.01$; ***$p < 0.001$; ****$p<0.0001$.

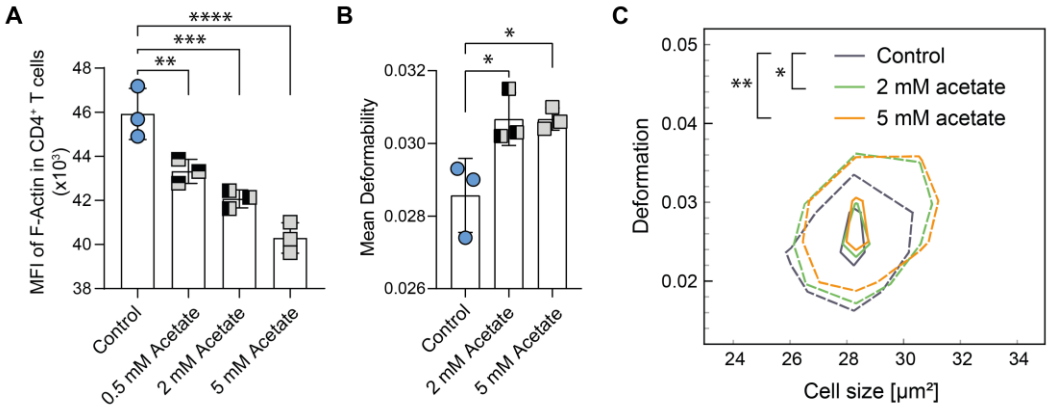

Fig. 2. Acetate exposure reduces F-Actin and affects T cell deformability.
(**A**) Flow cytometry analysis of mouse $CD4^+$ T cells shows a dose-dependent decrease in phalloidin-Alexa Fluor™-488 median fluorescence intensity (MFI). (**B**) A real-time deformability cytometry (RT-DC) of mouse $CD4^+$ T cells shows an increase in deformability upon 2 mM acetate and 5 mM acetate treatment (n = 3, $CD4^+$ T cells isolated from separate mice). (**C**) Overlay of control, 2 mM and 5 mM acetate treated $CD4^+$ T cell deformation and cell size. Data shown from one of three independent experiments (A) and one of two independent experiments (B, C) and expressed as mean ± SD. Statistical difference was determined by one-way ANOVA (A, B). Statistical analyses of panel C were carried out using a one-dimensional linear mixed model that incorporates fixed effect parameters and random effects to analyze differences between cell subsets and replicate variances, respectively. *p*-values were determined by a likelihood ratio test, comparing the full model with a model lacking the fixed effect term (C). *$p < 0.05$; **$p < 0.01$; ***$p < 0.001$; ****$p<0.0001$.

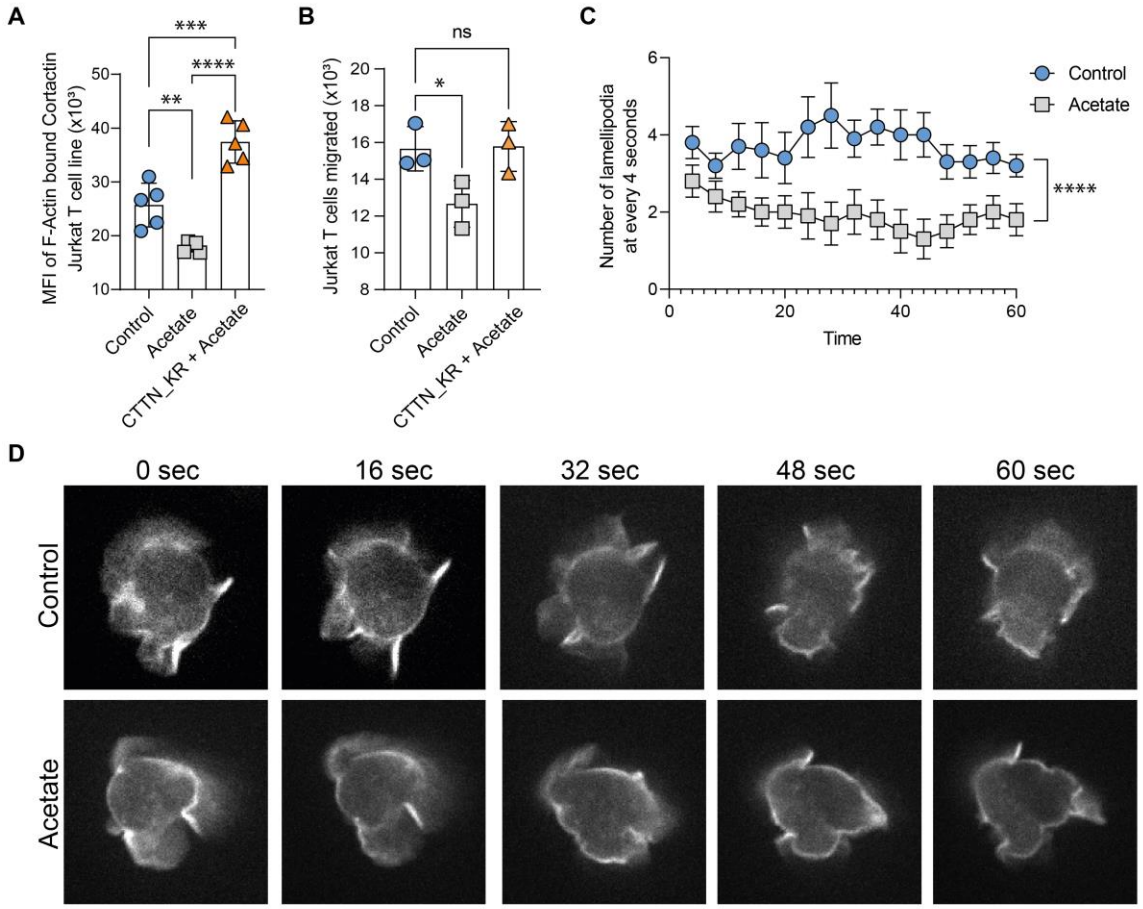

Fig. 3. Acetylation resistant cortactin rescues acetate-induced migration deficiency. (**A**) MFI of Förster Resonance Energy Transfer (FRET) from F-Actin bound cortactin in Jurkat T cells quantified by confocal scanning laser microscopy in control and acetate treatment, as well as in acetate treated Jurkat T cells expressing acetylation resistant cortactin (CTTN_KR). (**B**) Numbers of migrated Jurkat T cells in vitro trans-well assay of control, acetate treated, as well as acetate treated Jurkat T cells expressing acetylation resistant cortactin (CTTN_KR). (**C**) Numbers of lamellipodia per 4-second time points in LifeAct-mScarlet expressing Jurkat T cells upon control and acetate treatment (n = 10 cells). (**D**) Representative still images of control and acetate treated LifeAct-mScarlet expressing Jurkat T cells at 0, 16, 32, 48, and 60th seconds (for full movie see Movie S1). Data shown from one of three independent experiments (A, B) and one of two independent experiments (C, D) and expressed as mean ± SD. Statistical difference was determined by one-way ANOVA (A, B) and area under the curve analysis (C). *$p < 0.05$; **$p < 0.01$; ***$p < 0.001$; ****$p<0.0001$.

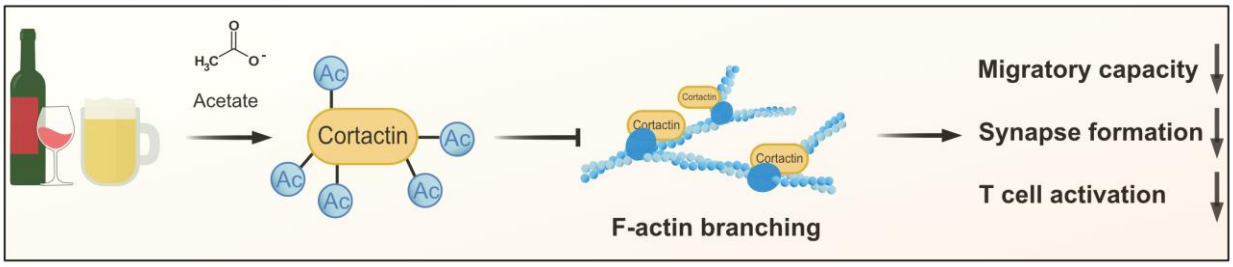

Fig. 4. Overview of the mode of acetate's action on T cell F-Actin reorganization.
Alcohol consumption results in accumulation of acetate in lymphoid organs, increases acetylated cortactin levels in T cells. This results in reduced F-Actin branching and consequently reduced migratory capacity, synapse formation, and activation.